ChemPubSoc Europe

DOI: 10.1002/chem.201xxxxxx

CHEMISTRY
A European Journal
Full Paper

Polyoxometalate reactivity

Molecular origin of the hydrolytic activity and fixed regioselectivity of a Zr(IV)-substituted polyoxotungstate as artificial protease

Karen Stroobants[a], Vincent Goovaerts[a], Gregory Absillis[a], Gilles Bruylants[b], Eva Moelants[c], Paul Proost[c] and Tatjana N. Parac-Vogt*[a]

Abstract: A multi-technique approach has been applied in order to identify the thermodynamic and kinetic parameters related to the regioselective hydrolysis of human serum albumin (HSA) promoted by the Wells-Dawson polyoxometalate (POM) $K_{15}H[Zr(\alpha_2\text{-}P_2W_{17}O_{61})_2]$. Isothermal Titration Calorimetry (ITC) studies indicate that up to four POM molecules interact with HSA. While the first interaction site is characterized by a 1:1 binding and an affinity constant of $3\cdot10^6$ M^{-1}, the three remaining sites are characterized by a lower global affinity constant of $6\cdot10^5$ M^{-1}. The higher affinity constant at the first site is in accordance with a high quenching constant of $2.2\cdot10^8$ M^{-1} obtained for fluorescence quenching of the Trp214 residue located in the only positively charged cleft of HSA, in the presence of $K_{15}H[Zr(\alpha_2\text{-}P_2W_{17}O_{61})_2]$. In addition, Eu(III) luminescence experiments with an Eu(III) POM analogue have shown the replacement of water molecules in the first coordination sphere of Eu(III) due to binding of the metal ion to amino acid side chain residues of HSA. All three interaction studies are in accordance with a stronger POM dominated binding at the positive cleft on the one hand, and interaction mainly governed by metal anchoring at the three remaining positions on the other hand. Hydrolysis experiments in the presence of $K_{15}H[Zr(\alpha_2\text{-}P_2W_{17}O_{61})_2]$ have demonstrated regioselective cleavage of HSA at the Arg114-Leu115, Ala257-Asp258, Lys313-Asp314 or Cys392-Glu393 peptide bonds. This is in agreement with the interaction studies as the Arg114-Leu115 peptide bond is located in the positive cleft of HSA and the three remaining peptide bonds are each located near an upstream acidic residue which can be expected to coordinate to the metal ion. A detailed kinetic study has evidenced the formation of additional fragments upon prolonged reaction times. Edman degradation of the additional reaction products has shown that these fragments result from further hydrolysis at the initially observed cleavage positions, indicating a fixed selectivity for $K_{15}H[Zr(\alpha_2\text{-}P_2W_{17}O_{61})_2]$.

Introduction

As the unraveling of the structure and function of proteins will lead to a better understanding of biochemical processes occurring in organisms and therefore result in more targeted drug therapy, protein structure determination is of major importance in biomedical research nowadays. Unfortunately, the use of X-ray crystallography, which is the most commonly used method to study the three-dimensional structure of proteins, is limited by the fact that a significant amount of proteins cannot be crystallized. Although this is avoided when NMR spectroscopy is used, in this case a millimolar concentration of a non-aggregated protein solution is needed. Furthermore, only limited success with NMR has been reported for the analysis of fluctuating protein states. Alternative methods study protein fragments rather than the full protein and thus require protein hydrolysis into more manageable peptides which can be traced back to the original protein structure. With a half-life of up to 600 years for peptide bond hydrolysis in the absence of a catalyst, the design of efficient protein hydrolyzing agents is a very challenging task.[1] Furthermore, most biochemical

[a] *K. Stroobants, V. Goovaerts, Dr. G. Absillis and Prof. Dr. T. N. Parac-Vogt*
Department of Chemistry
KU Leuven
Celestijnenlaan 200F, B-3001 Leuven, Belgium
Fax: (+)32 16 327992
E-mail: tatjana.vogt@chem.kuleuven.be

[b] *Dr. G. Bruylants*
Ecole polytechnique de Bruxelles
Université Libre de Bruxelles
avenue F.D. Roosevelt 50, B-1050 Bruxelles, Belgium

[c] *Dr. E. Moelants and Prof. Dr. P. Proost*
Department of Microbiology and Immunology
KU Leuven
Minderbroedersstraat 10, B-3000 Leuven, Belgium

Supporting information for this article is available on the WWW under http://www.chemeurj.org/ or from the author.

procedures require a high selectivity, depending on the preferred fragment size.

Currently used proteases can be divided into two classes, proteolytic enzymes and chemical agents. Proteolytic enzymes, with trypsin as the best known example, exhibit high catalytic powers but their use is limited to the stability window of the enzyme itself and their fixed selectivity. Moreover, since the active site of proteases has not been designed to fit native rigid structures, globular proteins are rather resistant to proteolysis at physiological conditions.[2] In addition, the use of an excess of protease or incubation at prolonged reaction times often leads to degradation of the protein up to its free amino acid components. As an alternative the chemical agent cyanogen bromide is often used under conditions where trypsin is inactive. However, cyanogen bromide requires harsh reaction conditions and causes side chain modifications which should be avoided.[3] Therefore new agents that operate under mild conditions and have tunable selectivity would greatly improve the applicability of the methods used in proteomics and related fields. One promising strategy is the use of limited proteolysis approaches to probe conformational features of globular proteins, however, these reactions have to be timed very precisely to avoid degradation into many small fragments.[4] Another often reported approach is the use of metal ions as reactive centers for peptide bond cleavage. Although numerous reports on oligopeptide and protein hydrolysis by metal ions and their complexes can be found in literature, only few examples were reported to be selective[5]. In a first approach, the metal complexes coordinate to either specific side chains or to the protein backbone. So far, the best results were obtained with Pd(II)[6] or Pt(II)[7] salts and their complexes which coordinate to the amino acid side chains of His and/or Met residues. In a second approach a Co(III) cyclen conjugate was tethered via a very tedious procedure to a peptide with known affinity for myoglobin, which consequently was cleaved at two peptide bonds.[8] In a last approach, mimicking of a natural peptidase active site by attachment of a Cu(II) cyclen complex to polystyrene resulted in hydrolysis of myoglobin, ovalbumin and bovine and human serum albumin.[9] Despite the remarkable selectivity exhibited by some of these complexes most of them have low activity at physiological pH or require multi-step synthetic procedures that lead to irreversible modification of certain amino acid side chains. In a novel approach recently proposed by our group, polyoxometalate compounds, characterized by a specific size, shape and charge are used to provide specific interactions with the protein surface.[10]

Polyoxometalates (POMs) are a class of metal-oxygen clusters for which variations in molecular composition, size, shape, charge density, and redox potential lead to a broad diversity of physical and chemical properties.[11] The asset that nearly every molecular property can be altered has been the most important motivation for the use of POMs in biological applications.[12] Tuning of the POM properties can influence the recognition and reactivity of these structures towards biological macromolecules, which so far has led to the discovery of three kinds of potential therapeutic applications. The first type of activity covers the field of viral infections[13], a second type is related to their use as anti-tumor agents[14] and the third type of activity is found in the area of bacterial diseases[15]. Both the enhancement of effectiveness of certain antibiotics[15] and the antiviral activity[13] in the presence of POMs were shown to be related to interactions with proteins. Anti-tumor properties on the other hand have been credited to POM-directed binding with tumor DNA.[14] The biological activity of POMs has been studied extensively and their interaction with biomolecules was often proposed as the basic mechanism of their biological action. Consequent studies have focused on the molecular understanding of POM interactions with proteins[10a, 16], however, reactivity was not reported in any of these studies. Subsequently, our group has investigated and reported on the carboxyesterase[17], phosphodiesterase[18] and peptidase[19] activity of isopolyoxomolybdates and isopolyoxovanadates as well as on the interactions preceding these POM catalyzed hydrolysis reactions. While hydrolytic activity toward phosphodiester bonds was credited to incorporation of the substrate inside the POM structure[18c], hydrolysis of carboxyester and peptide bonds was shown to originate from the nucleophilic nature of the POM[17, 19a] which caused activation via polarization of the target bond. More recently, sequence selective hydrolysis of hen egg white lysozyme (HEWL) in the presence of oxomolybdate was observed at the Asp-X sequences Asp18-Asn19, Asp48-Gly49, Asp52-Trp53 and Asp101-Gly102 at pH 5.0 and 60 °C.[20] Although the hydrolysis of dipeptides and proteins in the presence of oxomolybdate and oxovanadate solutions represented the first example of peptide bond hydrolysis catalyzed by oxoanions, the kinetic lability of this group of compounds at physiological pH renders tuning of their selectivity and the broader applicability difficult. Alternatively, heteropolyoxotungstates have a well-defined structure and are known to be stable under physiological conditions. Since these structures are inactive as such, combining the protein binding POM structure with Lewis acidic metal centers was proposed.

Attempts to create artificial peptidases by incorporating different metals such as Ni(II), Cu(II), Co(III) and some lanthanides into the lacunary Wells-Dawson structure α_2-$K_{10}P_2W_{17}O_{61}\cdot 20H_2O$, however, did not result into catalytically active species.[21] It could be reasoned that the embedded metal loses most of its coordination sites while at the same time its Lewis acidity is decreased upon incorporation into the POM ligand. Consequently metals with higher coordination numbers and stronger Lewis acidity such as Ce(IV), Hf(IV) and Zr(IV), were selected for further metal-substituted POM design. Zr(IV)-substituted POMs were previously shown to be efficient catalysts in organic reactions such as Mukaiyama aldol and Mannich-type reactions[22], H_2O_2[23] and sulfide oxidation reactions[24], and the cyclization of citronellal[25]. Furthermore, several studies in our group have indicated that Zr(IV)-substituted POMs are efficient catalysts for peptide bond hydrolysis in dipeptide model systems.[21, 26] More importantly, the first example of metal-substituted POM induced protein hydrolysis was observed in the presence of a Ce(IV) Keggin type POM and hydrolysis of HEWL was achieved at the Trp28-Val29 and Asn44-Arg45 peptide bonds under physiological conditions.[10b] In a recent study, we reported on the hydrolysis of human serum albumin (HSA) in the presence of different Zr(IV)-substituted polyoxotungstates.[27] Hydrolysis was shown to occur at the peptide bonds Arg114-Leu115, Ala257-Asp258, Lys313-Asp314 and Cys392-Glu393 and higher reaction rates were observed for POMs with a higher negative charge, presumably due to the electrostatic nature of the interactions preceding reaction.

In order to gain insight into the factors that influence the interaction between Zr(IV)-substituted Wells-Dawson POMs and HSA, in the current paper we investigate the thermodynamic and kinetic parameters associated with HSA hydrolysis in the presence of $K_{15}H[Zr(\alpha_2\text{-}P_2W_{17}O_{61})_2]\cdot 25H_2O$ (**1**), which was found to be the

most reactive polyoxotungstate compound in our previous study.[27] A multi-technique approach combining Isothermal Titration Calorimetry (ITC), Trp fluorescence and Eu(III) luminescence spectroscopy was used to study the interaction between **1** and HSA at a molecular level. In addition, a detailed kinetic study was performed to investigate the factors influencing the catalytic selectivity of **1**. This study is the further step towards understanding the parameters leading to the regioselective interaction between POMs and proteins, which will allow for a more rational design of POMs as artificial proteases with tunable reactivity and selectivity.

Results and Discussion

In our recent study HSA was shown to be regioselectively hydrolyzed by a series of Zr(IV)-substituted POMs, among which **1** (Figure 1) was found to be the most efficient.[27] The 1:2 sandwich structure of **1** can be converted into other species under different concentration, pH, temperature and ionic strength conditions (Figure 1).[21, 28] Due to the free coordination sites at the Zr(IV) ion, the 1:1 species was proposed to be the active species in dipeptide bond hydrolysis.[21] Although the 1:1 species was not observed under the conditions used for protein hydrolysis experiments (physiological pH, as opposed to pH 5 for the dipeptide bond studies), several publications have described exchange between the 1:2 and 1:1 species in the presence of various substrates.[29] Therefore, it is plausible that in the presence of HSA, which offers multiple coordination possibilities for Zr(IV), the dissociation of 1:2 into the hydrolyticaly active 1:1 form may occur. In the presence of **1**, the selective cleavage of HSA at the Arg114-Leu115 (site 1), Ala257-Asp258 (site 2), Lys313-Asp314 (site 3) and Cys392-Glu393 (site 4) peptide bonds was reported. Interestingly, while site 1 is situated at a positive patch of the protein, negatively charged acidic residues were observed upstream of the three remaining hydrolyzed peptide bonds. Consequently, a model has been proposed in which the electrostatic interaction between positive patches of HSA with the negatively charged POM precedes hydrolysis at site 1, while anchoring of Zr(IV) to the acidic side chains is responsible for the hydrolysis at the remaining three sites.

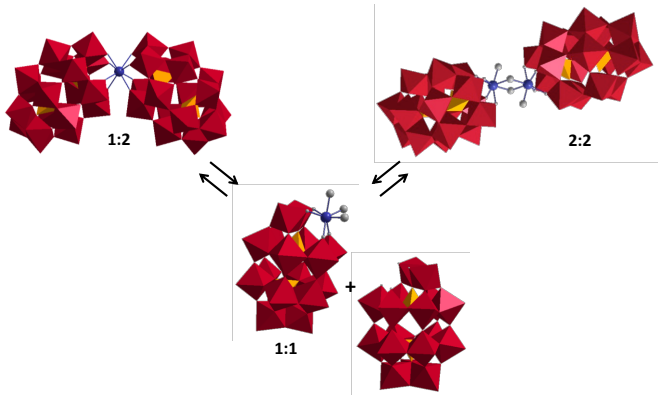

Figure 1. Schematic representation of $K_{15}H[Zr(\alpha_2\text{-}P_2W_{17}O_{61})_2]\cdot 25H_2O$ (**1** – on the left) and the species to which it can convert depending on its concentration, pH and temperature as well as the presence of ligands. WO_6 octahedrons are represented in red, PO_4 tetrahedrons in yellow, Zr(IV) in blue and coordinated waters in grey, respectively.

*Isothermal Titration Calorimetry study of the binding between HSA and **1**.* To further investigate the proposed model, the interaction of **1** with HSA was studied with Isothermal Titration Calorimetry (ITC). Since hydrolysis only occurs at elevated temperatures[27], titrations of **1** to HSA solutions were performed at room temperature assuring the integrity of the protein. As shown in Figure 2, the calorimetric titration curve obtained when adding **1** to HSA is divided into two parts and was fitted to a multiple sites binding model. The fittings resulted in a stoichiometry of 0.8±0.2 (≈1) and a binding constant K_a of $3\cdot10^6$ M^{-1} for the first part of the titration curve, and a stoichiometry of 2.8±0.2 (≈3) with a corresponding binding constant K_a of $6\cdot10^5$ M^{-1} for the second. The overall stoichiometry of about 4:1 (**1**:HSA) is in agreement with the results observed in SDS-PAGE experiments where four distinct cleavage positions occurring at the Arg114-Leu115, Ala257-Asp258, Lys313-Asp314, and Cys392-Glu393 peptide bonds were determined.[27]

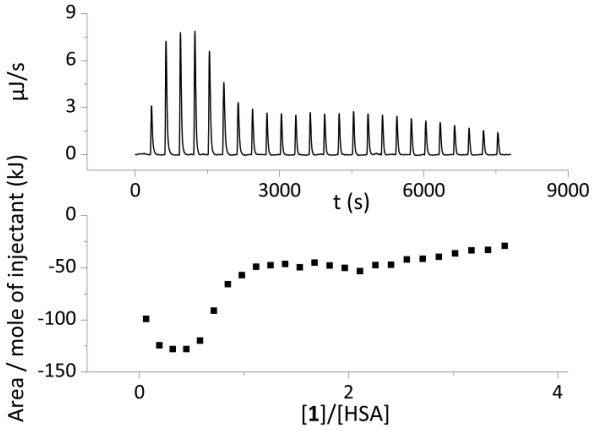

Figure 2. Thermogram (top panel) and isotherm (bottom panel) corresponding to binding of **1** to HSA. Aliquots of a solution of 250 µM of **1** were added to 20 µM solutions of HSA at 25 °C in 10.0 mM phosphate buffer (pH 7.4). Each peak in the top panels represents a single injection of **1** in the protein solution. In the bottom panel, a plot of the amount of heat liberated per mole of injectant as a function of the molar ratio to HSA is represented. A nonlinear least-square fit to a multiple site model was used to analyze the data.

The ITC data suggest that the affinity of **1** for one of the four sites is considerably higher than for the three remaining binding sites, which all three have comparable affinities. Considering the three-dimensional structure of HSA, binding near the Arg114-Leu115 peptide bond was proposed to be essentially driven by electrostatic interactions with the negatively charged POM structure as this peptide bond is located in the positive cleft of the protein which previously was identified as a POM binding position with high affinities in the order of 10^6 M^{-1}, which is in accordance with the here obtained value.[16a] For the interactions near the Ala257-Asp258, Lys313-Asp314 and Cys392-Glu393 peptide bonds a significant role of the Zr(IV) ion as such was anticipated due to its ability to anchor to the carboxylic function of Asp or Glu side chains.[27] However, the absence of interaction with the Zr(IV) salt $ZrCl_4$ (Figure S1), indicates a significant role of the POM skeleton also at these three positions. Titration of HSA with the lacunary Wells-Dawson (lacunary WD) POM, lacking the Zr(IV) metal center, at the other hand, resulted in a stoichiometry of 1:1

and binding constant of $1.5 \cdot 10^6$ M^{-1} (Figure S2). Since binding of the lacunary WD was previously reported to occur at the positive cleft of HSA[16a, 30], interaction at this same position is expected. In analogy, the stronger binding of **1** with 1:1 stoichiometry is proposed to also occur at this cleft, which contains the Arg114-Leu115 peptide bond. The K_a value which is in the order of 10^6 M^{-1} for interaction with **1** is comparable to the binding constants previously reported for Cu(II) and Ni(II) Wells-Dawson type POM binding to HSA. Competition experiments furthermore have indicated that, for both POMs, one of the interaction sites is located at the HSA positive cleft.[30] However, the stoichiometries for binding of the various POM complexes differ significantly. While 1:1 and 1:4 (HSA:POM) stoichiometries were observed for binding of the lacunary Wells-Dawson and **1**, respectively, stoichiometries of 1:1 and 1:3 were reported for Cu(II) and Ni(II)-substituted Wells-Dawson binding to HSA, respectively.[16c] Although the Cu(II) and Ni(II) ions both are small enough to reside in the vacant pocket created by the removal of one octahedron from the POM structure where they adopt a 5-fold coordination, their different binding was attributed to subtleties in the coordination geometry. It was proposed that small differences in the occupancy mode of the vacancy as well as in the presence or absence of Jahn-Teller distortions are able to cause considerable changes in the molecular interaction behavior.[16c] Since the Zr(IV) ion is much larger, a more significant difference in the binding mode to the POM vacancy can be expected to result in an even more pronounced effect on the POM interaction behaviour. The Zr(IV) ion sits on the POM vacancy in a 4-fold coordination and can be anticipated to interact more readily with proximal acidic residues and cause more profound changes on the POM interaction mode with other molecules, e.g. proteins. Apart from the influence of the nature of the metal ion, the different binding stoichiometries can alternatively be a consequence of the different size and charge of the complexes upon interaction with the protein substrate. While **1** initially is dissolved as a 1:2 sandwich structure with a negative charge of -16, Cu(II) and Ni(II) substitution can only result in a monomeric 1:1 POM, resulting in a smaller charge of -8. Furthermore, the larger size of the 1:2 sandwich species might result in interaction with more distant positive surface patches as opposed to those reachable upon binding of the 1:1 monomeric POMs.

The ITC experiments clearly indicate involvement of both the POM structure and Zr(IV) ion in the interaction with the HSA surface. Similarly, the trend in which the binding could be dominated by either the POM structure or by the incorporated Lewis acid ion was previously observed for Ce(IV)-Keggin interactions with HEWL.[10b] In this case, a higher affinity was anticipated for the electrostatic interaction at the positive surface near the Trp28-Val29 cleavage site as compared to the interaction at Asn44-Arg45 which was proposed to be driven by the anchoring of the Ce(IV) metal to the protein.[10b] In analogy with these results a stronger binding of **1** to HSA is proposed at the positively charged cleft, while the interactions between Zr(IV) and the coordinating carboxylate groups of the Asp and Glu side chains are suggested to dominate the interaction at the remaining three binding sites.

Titrations of HSA with $ZrCl_4$ were also performed, however, no interaction was observed (Figure S1) indicating that although Zr(IV) plays a significant role in the binding to HSA, it needs to be incorporated in the POM skeleton for efficient coordination to the protein surface. All discussed titrations show that interactions between **1** and HSA are exothermic processes (Figure 3). The negative sign of the interaction enthalpy $\Delta H°$ seems to indicate a net favorable redistribution of the hydrogen bond network between the species.[31] The unfavorable entropic contributions $\Delta S°$ on the other hand, are signature of a conformational change in the protein.[31]

Figure 3. Schematic diagram showing the thermodynamic signature of the

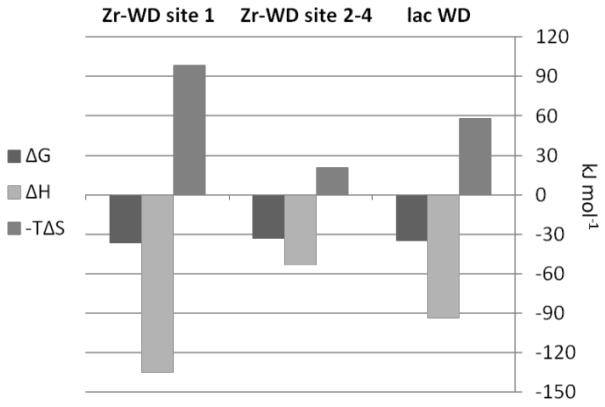

interaction between 1 (Zr-WD) / lacunary Wells-Dawson (lac WD) and HSA.

*Quenching of Trp fluorescence by **1**.* Since the HSA cleft, at which the Arg114-Leu115 peptide bond is located, contains the only Trp214 residue of the protein[32], fluorescence quenching was further used to study the interaction of **1** with HSA. In the performed steady state fluorescence experiments, the concentration of protein was kept constant (10^{-5} M), while the concentration of **1** (Figure 4) or lacunary POM (Figure S3) was increased stepwise from 0 to 10^{-5} M with increments of 10^{-6} M. The analysis of the results was done with the help of a derived Stern-Volmer equation [1]:

$$\log\frac{(F_0\text{-}F)}{F} = \log K_q + n \log[Q] \qquad [1]$$

where F_0 is the unquenched fluorescence intensity, F the fluorescence in the presence of the quencher and [Q] the concentration of the quencher. The main advantage of using this equation is the possibility of extracting the quenching constant (K_q) and the number of bound molecules (n). For the interaction of HSA with **1** and with the lacunary Wells-Dawson, n-values of 1.5 and 1.3, and quenching constants K_q of $2.2 \cdot 10^8$ and $5.7 \cdot 10^6$ M^{-1}, respectively, were calculated. It is notable that the quenching constant for binding of **1** is higher as compared to the quenching due to the presence of the lacunary Wells-Dawson. The fluorescence quenching in the presence of **1** as well as the calculated quenching constant strengthen the hypothesis that the single interaction at a higher affinity binding site occurs at the positive cleft of the protein, as this is also where Trp214 is located. The fluorescence quenching in HSA by POMs of Keggin, Wells-Dawson and Lindqvist type has previously been studied[16g, 30, 33] and n-values around 1 and quenching constants in the range between 10^4 to 10^6 M^{-1} were obtained. A higher quenching constant indicating a stronger interaction is observed for binding of **1** to HSA. This is in accordance with hydrolysis results where superior reactivity of Zr(IV)-substituted Wells-Dawson POMs as compared to Zr(IV)-substituted POMs of the Keggin and Lindqvist type was

observed,[10b] presumably as a result of its higher negative charge density and more favourable interaction with the HSA surface.

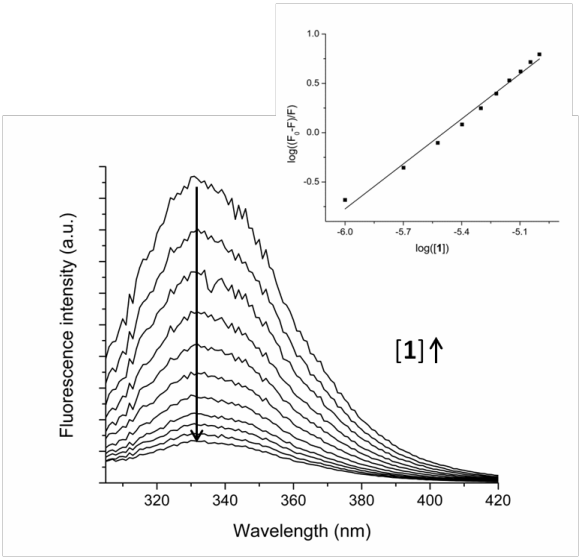

Figure 4. Emission fluorescence spectra of HSA in the absence and presence of different concentrations of **1** ([HSA]=10^{-5} M, pH = 7.4). From top to bottom, the concentration of POM was increased stepwise from 0 to 10^{-5} M with increments of 10^{-6} M. In the inset, the plot (R^2 = 0.988) of the derived Stern-Volmer equation is given.

Table 1. Calculated values of the fluorescence quenching constants for different Wells-Dawson type POMs.

POM	protein	K_q (M^{-1})	ref
lacunary WD	HSA	$5.72 \cdot 10^6$	This work
Zr(IV)-WD	HSA	$2.24 \cdot 10^8$	This work
Eu(III)-WD	HSA	$2.64 \cdot 10^7$	This work
lacunary WD	HSA	$4.10 \cdot 10^4$	[30]
Cu(II)-WD	HSA	$5.92 \cdot 10^4$	[30]
Ni(II)-WD	HSA	$1.15 \cdot 10^5$	[30]

Large differences are again observed between various metal-substituted Wells-Dawson type POMs. For comparison reasons, the interaction of HSA with the hydrolytically inactive Eu(III) Wells-Dawson POM analogue which was used in Eu(III) luminescence experiments (vide supra), was studied and a 1:1 interaction with quenching constant K_q of $2.6 \cdot 10^7$ M^{-1} was obtained. Thus, whereas quenching constants in the order of 10^4-10^5 M^{-1} were previously found for the Cu(II) and Ni(II) Wells-Dawson POMs[30], values in the order of 10^7-10^8 M^{-1} were obtained for the Eu(III)- and Zr(IV)-substituted Wells-Dawson POMs, respectively, by our group (Table 1). However, a difference of two orders of magnitude is also observed between the previously reported value of the quenching constant in the presence of the lacunary Wells-Dawson and the value we have obtained in this work. Although the reason for this discrepancy is not clear, the value for binding of **1** shows a significant increase as opposed to other values, even taking this into account. The observed differences in the K_q values presumably are a consequence of the larger size and charge of the dissolved 1:2 Zr(IV)/Eu(III) sandwich complex as opposed to the 1:1 monomeric Cu(II)/Ni(II) structure, as previously discussed.

*Interaction between HSA and **1** studied by Eu(III) luminescence spectroscopy.* Since apart from the electrostatic POM driven interactions, metal-dominated binding was proposed to play an important role, Eu(III) luminescence experiments were used to study POM binding to HSA. The Zr(IV) ion cannot be used for this purpose as it is not luminescent, therefore the Eu(III)-substituted Wells-Dawson POM $K_{13}(H_2O)[Eu(H_2O)_{3/4}(\alpha_2\text{-}P_2W_{17}O_{61})_2] \cdot 2KCl \cdot nH_2O$ was synthesized.[34] In an attempt to observe protein hydrolysis with this complex, 100 equivalents were added to a HSA solution and incubated at 60 °C and pH 7.4 during 7 days. Even after this prolonged reaction time, no hydrolysis fragments were observed and it was concluded that the complex is inactive towards protein hydrolysis. Therefore, it is a good model for structural studies on metal-substituted 1:2 POM binding. Time-resolved luminescence measurements in H_2O and D_2O allowed to calculate the number of bound water molecules to the Eu(III) metal incorporated in the Wells-Dawson structure using equation [2]:

$$q(Eu) = 1.11(\Delta k_{obs} - 0.31) \quad [2]$$

where q represents the number of bound water molecules and Δk_{obs} is equal to $(1/\tau_{H2O}) - (1/\tau_{D2O})$ with τ the lifetime of the $^5D_0$ excited state of the Eu(III) ion in the respective solvent.[35] For the dissolved Eu(III)-substituted Wells-Dawson, which is synthesized as a 1:2 complex analogous to **1**, lifetimes of 0.23 ± 0.01 ms in H_2O and 2.97 ± 0.01 ms in D_2O were calculated in the absence of protein and a coordination of 4 water molecules around Eu(III) was derived. This result is in accordance with previously reported lifetime values.[16g] Since 4 water molecules are bound to the Eu(III) metal it is likely to assume that the 1:2 species in solution is converted to the 1:1 form at 10^{-4} M concentrations. The absence of species with different lifetimes even indicates full conversion of the Eu(III)-substituted Wells-Dawson to the 1:1 form. It can be assumed that also for **1** a shift to the 1:1 species occurs at lower concentrations as was previously proposed.[27] However, speciation differences for Eu(III)- compared to Zr(IV)-substituted Wells-Dawson POMs should be considered.

In the presence of 0.1 to 1 equivalents of HSA a first set of lifetimes of 0.23 ± 0.01 ms in H_2O and of 2.97 ± 0.01 ms in D_2O was again associated to the tetra hydrated Eu(III) ion in the 1:1 POM species, while a second set of lifetimes of 0.82 ± 0.01 ms in H_2O and of 1.07 ± 0.01 ms in D_2O was associated with a fully dehydrated form since the hydration number for this complex resulted in a negative value, suggesting that all four water molecules had been replaced by HSA residue interactions. The fact that all water molecules are removed from the coordination sphere of the metal centre upon protein binding can explain the lack of reactivity observed in the presence of the Eu(III) Wells-Dawson. The Zr(IV) metal ion with higher maximal coordination number can coordinate an additional water molecule and might not be fully dehydrated allowing remaining coordinated water to act as a nucleophile in the hydrolysis reaction. In an alternative mechanism, external water from the solvent can also fulfill this role. In addition to its higher coordination number, the Zr(IV) ion also has a considerably higher Lewis acidity as compared to the Eu(III) ion which can also explain its higher reactivity independent of the water delivery mechanism.

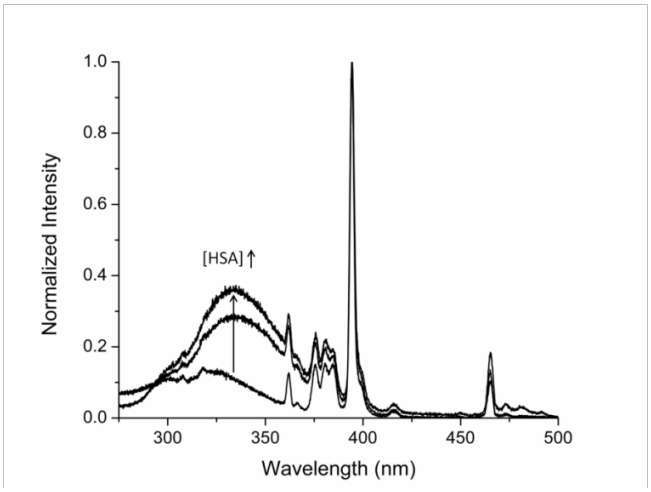

Figure 5. Excitation spectra of the Eu(III) Wells-Dawson POM (10^{-4} M) in the presence of 0, 10^{-5} and 10^{-4} M of HSA (bottom to top). The emission was monitored at 613 nm.

Apart from time-resolved experiments, steady state luminescence measurements were carried out. The excitation spectrum of the Eu(III)-substituted Wells-Dawson POM in solution is characterized by excitation lines at 362 nm ($^5D_4 \leftarrow {}^7F_0$), 375, 380 and 384 nm (combination of $^5G_2$, $^5L_7$, $^5G_{3\text{-}6} \leftarrow {}^7F_{0,1}$), 394 nm ($^5L_6 \leftarrow {}^7F_0$), 416 nm ($^5D_3 \leftarrow {}^7F_{0,1}$), 428 nm ($^5D_3 \leftarrow {}^7F_2$), 465 nm ($^5D_2 \leftarrow {}^7F_0$), 473 nm ($^5D_2 \leftarrow {}^7F_1$) and 487 nm ($^5D_2 \leftarrow {}^7F_2$) and a weak broad metal-to-charge transfer (LMCT) band from 300 to 370 nm. The latter is attributed to a charge transfer between the oxygen and tungsten atoms of the POM ligand (O → W).[16f] Upon addition of HSA, the number of excitation peaks remains unchanged as can be seen in Figure 5, however, the position of the LMCT band shifts to higher wavelengths and increases in intensity. The shifting of the maximum of the LMCT band is indicative of interaction between the Eu(III) metal and the protein, which is in accordance with the time-resolved measurements.[10a, 36]

The emission spectrum of the Eu(III) Wells-Dawson exhibits four bands with strong intensities at 580, 593, 613 and 700 nm (Figure 6). While the three latter are expected to be strong as they are associated with the $^5D_0 \rightarrow {}^7F_1$, $^5D_0 \rightarrow {}^7F_2$ and $^5D_0 \rightarrow {}^7F_4$ transitions[37], the high intensity of the $^5D_0 \rightarrow {}^7F_0$ transition is unusual and the reason for this peculiarity is unclear. The Eu(III) characteristic luminescence is highly dependent on the local environment of the ion and whereas the transition at 593 nm ($^5D_0 \rightarrow {}^7F_1$) has a magnetic-dipolar origin and should not be strongly affected by the environment of the Eu(III) ion, the transition at 613 nm ($^5D_0 \rightarrow {}^7F_2$) is highly affected due to its electric-dipolar origin. In addition, this $^5D_0 \rightarrow {}^7F_2$ transition is hypersensitive and its intensity increases as the site symmetry decreases, rendering it as an excellent structural probe. In combination with the $^5D_0 \rightarrow {}^7F_1$ transition which serves as a reference, the I_{613}/I_{593} ratio gives a good indication of the changes in the local environment of the Eu(III) ion. The calculated value for the Eu(III) Wells-Dawson POM in the absence of protein is 2.33, while the value obtained for a solution containing Eu(III) Wells-Dawson POM with HSA in a 1:1 ratio is 3.80. This represents an increase by a factor of 1.63, indicating that the Eu(III) ion is positioned in a different environment with lower symmetry in the presence of HSA. The inset of Figure 6 shows the relative intensity increase of the $^5D_0 \rightarrow {}^7F_1$ (593 nm), $^5D_0 \rightarrow {}^7F_2$ (613 nm) and $^5D_0 \rightarrow {}^7F_4$ (700 nm) transitions in the presence of increasing amounts of HSA, almost a 2-fold increase is observed for the most intense $^5D_0 \rightarrow {}^7F_2$ transition at 613 nm. The increase in intensity can be explained by the substitution of water molecules bound to the Eu(III) ion by HSA side chain residues. The luminescence of the Eu(III) ion is highly quenched by bound water molecules due to the deactivation of the $^5D_0$ excited state by coupling with OH oscillators. When water is substituted for protein side chain residues, this deactivation and hence, the quenching of the Eu(III) luminescence is decreased. As a result, higher intensities can be detected. Similar observations were reported for the luminescence spectra of $[EuW_{10}O_{36}]^{9-}$ in the presence of BSA and HSA.[16e-g]

Figure 6. Steady state emission spectra for the Eu(III) Wells-Dawson POM (10^{-4} M) upon increasing concentrations of HSA (0-10^{-4} M) in phosphate buffer (1.0 mM - pH 7.4). Excitation took place at a wavelength of 393 nm. The relative

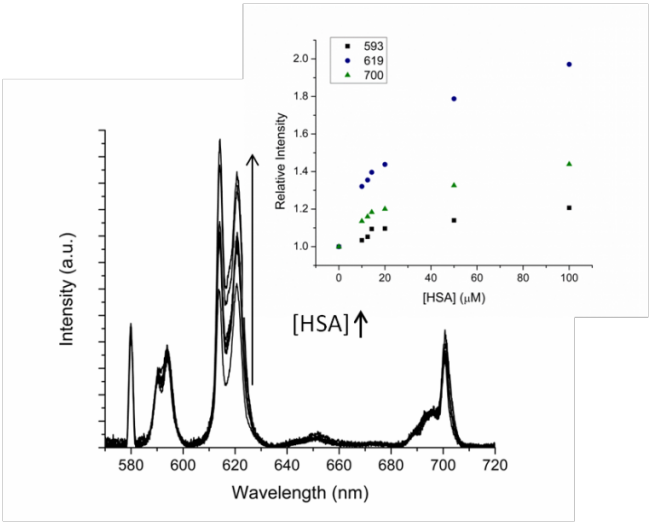

intensity increase for the 3 main emission transitions: $^5D_0 \rightarrow {}^7F_1$ (593 nm, black squares), $^5D_0 \rightarrow {}^7F_2$ (619 nm, blue dots) and $^5D_0 \rightarrow {}^7F_4$ (700 nm, green triangles) is plotted in the inset.

From the data of the emission spectra, an association constant for the Eu(III) Wells-Dawson:HSA interaction was estimated by the use of equation [3]:

$$\log[(I_{sam}-I_{bl})/I_{sam}] = \log K_a + n \log [P] \qquad [3]$$

where I_{sam} is the intensity of the sample, I_{bl} the intensity of the sample in the absence of protein, K_a the association constant, n the number of binding molecules and [P] the concentration of protein added. For the interaction with HSA a K_a value of $1.07 \cdot 10^3$ M^{-1} was estimated. This value is lower compared to the values which were obtained by ITC, most likely due to the different POM-imbedded metal ions as well as the different techniques used in these two studies. As the Zr(IV) ion has a considerably greater Lewis acidity as compared to the Eu(III) ion, a larger K_a can be anticipated. Nonetheless, the luminescence experiments clearly show metal binding to HSA for the Eu(III)-substituted Wells-Dawson, as replacement of coordinated water molecules with protein residue interactions was observed both with time-resolved and steady state luminescence experiments.

*Secondary HSA fragmentation in the presence of **1.*** The interaction studies described above were performed upon mixing of **1** and HSA , and thus are representative for the initial interaction leading to hydrolysis at the Arg114-Leu115 (site 1), Ala257-Asp258 (site 2), Lys313-Asp314 (site 3) and Cys392-Glu393 (site 4) peptide bonds, which resulted in 8 fragments with Mw of ca. 53, 44, 37, 35, 31, 29, 22 and 13 kDa.[27] For the sake of simplicity, the fragments from the regioselective hydrolysis of HSA in the presence of **1** will be marked with letters from A to H and contain following sequences: A (Leu115-Leu583), B (Lys1-Cys392), C (Asp258-Leu583), D (Lys1-Lys313), E (Asp314-Leu583), F (Lys1-Ala257), G (Glu393-Leu583) and H (Lys1-Arg114) (Figure 9).[27] After prolonged incubation of HSA with **1**, additional fragments were observed on the gel and this was further investigated. Therefore additional SDS-PAGE experiments were performed which have led to a more detailed kinetic analysis of the HSA hydrolysis in the presence of **1**. The hydrolysis of 0.02 mM of HSA in the presence of increasing amounts of **1** from 0.5 to 200 equivalents was investigated at pH 7.4 (phosphate buffer, 10.0 mM) and 60 °C. For each ratio, samples were taken at different time increments during 4 days and the progress of the reaction was visualized by SDS-PAGE and subsequent silver staining (Figure S4).

Measuring the intensity of the original HSA band allowed calculation of the residual protein concentration, which was plotted as a function of time. The exponential shape of this plot (shown for [**1**]=0.75 mM, Figure S5a) as well as the linear trend for the plot of the logarithm of the HSA concentration as a function of time (Figure S5b), are indicative of first-order reaction kinetics. Fitting the data to first-order equations resulted in a rate constant of $19.5 \cdot 10^{-3}$ h^{-1} and a half-life of 35.6 h for the hydrolysis of HSA in the presence of 0.75 mM of **1**, which is a significant improvement as compared to the half-life values for the uncatalyzed hydrolysis of peptide bonds that can be up to a few hundred years.[1] Yashiro and coworkers reported comparable rate constants between $16 \cdot 10^{-3}$ h^{-1} and $44 \cdot 10^{-3}$ h^{-1} for the hydrolysis of BSA, which is homologous to HSA in the presence of several Zn(II) complexes.[38] Although a lower reagent:protein ratio was used in the Zn(II) study, the reactions were performed in strongly alkaline solutions (pH 11), while hydrolysis in our work occurred at physiological pH.

Values of k_{obs} ranging from $0.3\ 10^{-3}$ h^{-1} to $37.6\ 10^{-3}$ h^{-1} for **1**:HSA ratios of 1:2 to 200:1 were obtained in a similar way. The obtained rate constants k_{obs} were plotted as a function of the concentration of **1** and fitted to a pseudo-Michaelis-Menten model (equation [4]), as is shown in Figure 7.[39]

$$k_{obs} = \frac{k_{max} * [\mathbf{1}]}{K_M + [\mathbf{1}]} \qquad [4]$$

where k_{obs} is the observed first-order reaction rate constant, k_{max} is the maximal observed rate constant and K_M is the Michaelis constant which represents the concentration of **1** for which k_{obs} equals $k_{max}/2$. From equation [4] a maximal rate constant k_{max} of $44.6 \cdot 10^{-3}$ h^{-1} ($t_{1/2}$ of 15.5 h) and Michaelis constant K_M of 0.83 mM (or 41.5 equivalents) were calculated for the hydrolysis of HSA by **1** at pH 7.4 and 60 °C. Apart from the previously reported HSA sequences (A-H), hereafter referred to as primary fragments, protein bands at the estimated masses of ca. 7, 10, 15, 17, 23 and 32 kDa, hereafter referred to as secondary fragments, were observed both at higher concentrations of **1** (Figure S4) and/or upon incubation at increased reaction times (Figure 8). The primary (A-H) as well as the secondary fragments are indicated on the SDS-PAGE gels in Figure 8.

Figure 7. Plot of the observed rate constant as a function of the concentration of

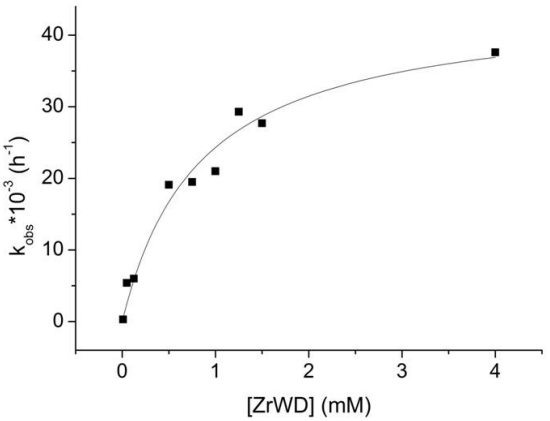

1 for the hydrolysis of HSA (0.02 mM) at pH 7.4 (phosphate buffer, 10.0 mM) and 60 °C, fitted to pseudo Michaelis-Menten equation [1].

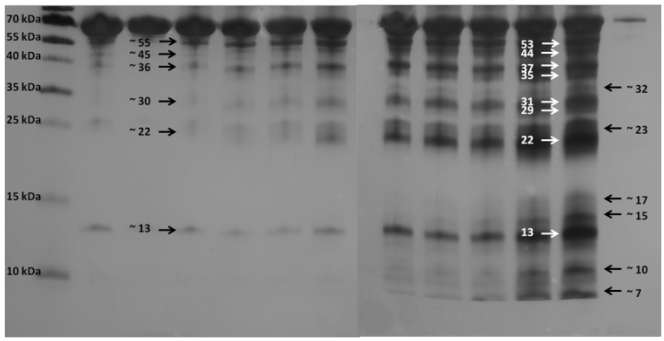

Figure 8 SDS-PAGE gel of HSA hydrolysis in the presence of 10 equivalents of **1** at 60 °C and pH 7.4 (phosphate buffer, 10.0 mM) at increasing reaction times up to 5 days (8, 24, 32, 48, 56, 72, 80, 96, 104, 120 and 128 h from left to right). The black arrows in the left panel show the estimated masses of the primary fragments (BioRad ImageLab analysis software). In the right panel, the white arrows indicate the calculated masses of the primary fragments which were obtained by Edman degradation, while the black arrows represent the estimated masses of the secondary fragments (BioRad ImageLab analysis software).

Selectivity of the secondary fragmentation. SDS-PAGE gels of reactions leading to secondary fragmentation (10 eq. of **1** after 5 days of incubation at 60 °C and pH 7.4) were blotted to a PVDF membrane and the fragments were analyzed by Edman degradation of a minimum of 5 amino acid residues. Analysis of all the secondary fragments revealed that they contained either the NH_2-terminal sequence of HSA (and therefore were the result of secondary hydrolysis of fragments F, D, and/or B) or fragments having an Asp314Val315Cys316Lys317Asn318 or Asp258Leu259Ala260Lys261Tyr262 NH_2-terminal sequence, meaning that they resulted from hydrolysis of fragments E and C respectively (Figure 9).

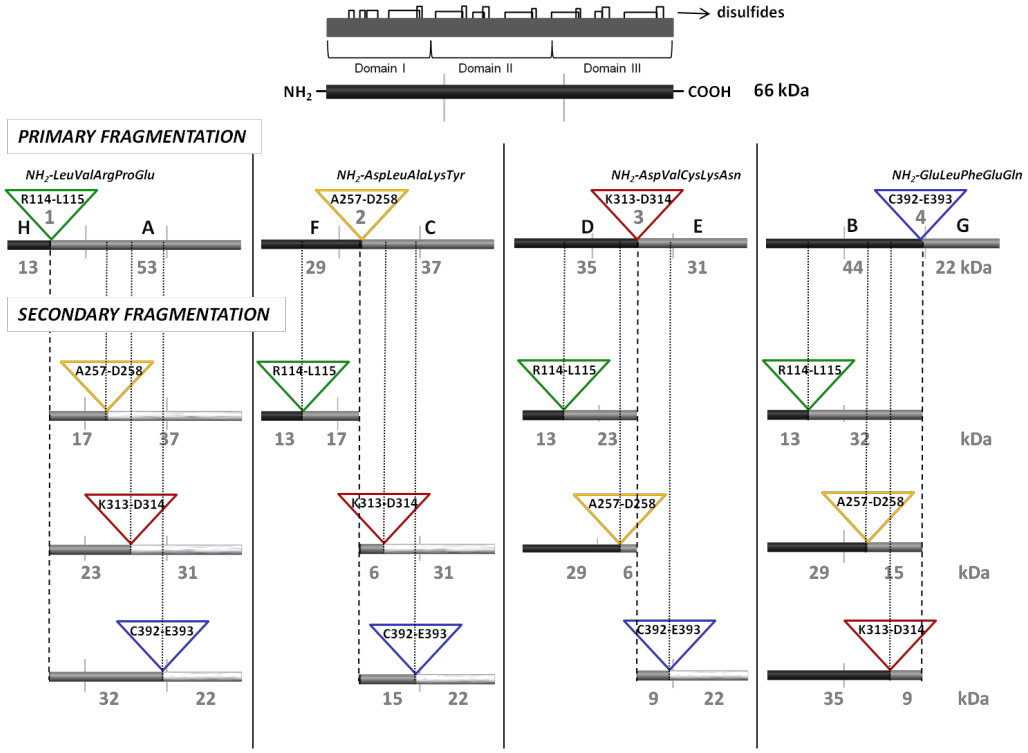

Figure 9. Schematic representation of HSA, with mainly α-helical structure content and 17 disulfide bridges. During the primary HSA fragmentation in presence of **1** cleavage occurs at four distinct cleavage sites. Fragments with sizes of 13/54, 29/37, 35/31 and 45/22 kDa are obtained. Upon prolonged incubation times or higher concentrations of **1**, primary fragments are further hydrolyzed at either of the remaining intact peptide bonds (secondary fragmentation).

As no fragments with an NH_2-terminal sequence different from the ones previously obtained for fragments A to H were identified, it is clear that the secondary fragmentation does not occur at the intact HSA but at the fragments that were produced during the initial stages of the hydrolysis.

Based on the data from SDS-PAGE and Edman degradation the cleavage sites of the secondary fragmentation could be estimated as follows. Further hydrolysis of HSA at the peptide bonds of sites 1-4 (Arg114-Leu115, Ala257-Asp258, Lys313-Asp314 or Cys392-Glu393) would result in additional peptides with molecular masses of ca. 6, 9, 15, 17, 23 and 32 kDa, as is schematically shown in Figure 9. These values are in good agreement with the estimated masses of the secondary fragments observed on the SDS-PAGE gel in Figure 8. Since several pathways shown in Figure 9 would lead to production of the same fragments, it is likely that secondary hydrolysis did not occur at all 8 fragments. For example, considering only secondary hydrolysis at the Ala257-Asp258 (in fragment A, D and/or B) and Lys313-Asp314 (in fragment A, C and/or B) peptide bonds, as observed by the Edman sequences Asp314Val315Cys316Lys317Asn318 and Asp258Leu259-Ala260Lys261Tyr262, would result in the full cleavage pattern, apart from the 32 kDa fragment. The presence of this fragment on the SDS-PAGE gel can be explained either by the hydrolysis of fragment A at the Cys392-Glu393 peptide bond (site 4) or by the hydrolysis of fragment B at the Arg114-Leu115 peptide bond (site 1), however, the corresponding NH_2-terminal sequences were not observed in the Edman degradation experiments. Interestingly, although additional cleavage positions might be expected upon dissociation of the HSA structure as some additional regions will become solvent accessible, no other sequences were obtained even after several rounds of NH_2-terminal Edman degradation analysis. This indicates that the selectivity of **1** remains fixed, as only hydrolysis at four sites (sites 1-4) was observed, either on the intact HSA or in the fragments produced upon primary hydrolysis.

The primary fragmentation was previously shown to be directed by interactions between the negative POM / positive metal at the one hand and the protein surface charges at the other. This was confirmed by ITC, Trp fluorescence and Eu(III) luminescence experiments as reported above. The balance of positive and negative charge at the HSA surface thus determines the regioselectivity of **1** and this could be expected to change after primary peptide bond cleavage, leading to secondary fragmentation at different positions. However, all of the primary hydrolysis sites are located in loops or α-helices connecting domains or subdomains of the HSA structure which are internally stabilized by disulfide bridges. Due to the large amount of in total 17 of these disulfides[40], large parts of the protein can be expected to remain folded even after primary fragmentation. The Arg114-Leu115 binding site is located in a loop that connects the Ia and Ib subdomains of the HSA structure[40]. As a result hydrolysis at this position will separate the Ia subdomain from the rest of the structure. Since the Ala257-Asp258 bond is located in the IIa subdomain of HSA[40] hydrolysis at this peptide bond will separate domain I together with part of subdomain IIa from the rest of domain II and domain III. The Lys313-Asp314 site is located in subdomain IIb[40] in a loop separating the IIa subdomain from the IIb subdomain. The last site at the Cys392-Glu393 peptide bond lies in the first α-helix of subdomain IIIa.[40] Hydrolysis of this bond would separate domain III from the rest of the structure, unless the disulfide bridge between Cys392 and Cys438 remains unbroken upon hydrolysis by **1**. In the latter case, the cleavage of this peptide bond does not cause effective separation in the HSA structure. Thus, while hydrolysis at site 1 and 4 results in conservation of two out of three domains, II & III and I & II, respectively, only one domain, I or III, is left intact upon respective cleavage at site 2 or 3, which both are located in domain II. Moreover, a study of Rüker

et al., where the separate HSA domains I, II and III were expressed, demonstrated that these domains exhibit secondary and tertiary structures comparable to that found in wild type HSA.[41] Therefore, it can be anticipated that secondary fragmentation of the similarly folded protein domains will follow the same binding mode and reaction mechanism than is observed for the primary hydrolysis of HSA.

These results indicate that the regioselective interaction preceding hydrolysis, which was supported here by ITC, Trp fluorescence and Eu(III) luminescence data, is preserved also at higher concentrations of **1** and after prolonged incubation times. Since the loss of selectivity upon increased reaction times or upon addition of excess of the reagent are major drawbacks of naturally occurring proteases, this is a very interesting asset of the proposed POM based artificial proteases. In addition, the autodegradation of natural proteases is avoided by this method. Futhermore, the electrostatic protein recognition is interesting in the light of structure determination of globular proteins at physiological conditions in particular. Previously proposed limited proteolysis approaches for structure determination are based on the use of classical proteolytic enzymes which can undergo self-digestion and in addition, the dynamic state recognition basis of this technique requires a delicate control of the catalyst concentration, temperature and reaction times to avoid fragmentation into many small peptides.[2, 4] These disadvantages are avoided by use of the here proposed POM-based structures, which recognize protein regions with specific electrostatic characteristics and retain their selectivity even in the presence of large excess and/or upon increased reaction times.

Conclusion

This study gives further insight and reveals the parameters which drive the recognition between a Zr(IV) Wells-Dawson POM and HSA, resulting in selective cleavage of the protein. The binding of **1** to HSA is governed by two factors: an electrostatic interaction between the POM skeleton and the binding cleft of the protein, and three slightly weaker interactions resulting from the anchoring of Zr(IV) ion to HSA side chains. These results were further confirmed by Trp fluorescence and Eu(III) luminescence experiments which showed binding of the POM at the Trp214 found in the binding cleft of HSA, and interactions of a Eu(III) Wells-Dawson analogue with HSA side chains. Both the calorimetric and spectroscopic studies thus support a mechanism of balanced POM / metal electrostatic interactions with the protein surface as driving force for the observed reactivity. The fragmentation extent of HSA can be tuned by either changing the concentrations of **1** or the incubation time. The secondary fragmentation that occurs at high concentration or after prolonged incubation times was found to occur at the same sequences as the primary fragmentation, thus indicating that regioselectivity is preserved independent of the reaction time or amount of POM used. This a very interesting asset considering the fact that classical sequence selective proteases often suffer from the loss of selectivity when used in excess or upon prolonged incubation times, and are not always reactive toward globular proteins under physiological pH conditions.

Experimental Section

Synthesis

$K_{10}[\alpha_2\text{-}P_2W_{17}O_{61}]\cdot 20H_2O$[42], $K_{15}H[Zr(\alpha_2\text{-}P_2W_{17}O_{61})_2]\cdot 25H_2O$[43] and $K_{13}(H_2O)[Eu(H_2O)_{3/4}(\alpha_2\text{-}P_2W_{17}O_{61})_2]\cdot 2KCl\cdot nH_2O$[34] were prepared by the published procedures. Human serum albumin (HSA) was purchased from Sigma-Aldrich in the highest available purity and was used without further purification.

Isothermal titration calorimetry

All experiments were performed on a nano-ITC 2G from TA Instruments (New Castle, Delaware, USA). In a typical experiment a protein solution (±25 μM) in the 1.0 mL calorimeter cell was titrated by 25 successive injections of 10 μL (5 μL for the first injection) of a ligand solution (± 250 μM).

Fluorescence spectroscopy

Steady state fluorescence experiments were recorded on a Photon Technology Quanta Master QM-6/2005 spectrofluorimeter. Spectra were recorded for solutions containing 10^{-5} M HSA, the concentration of 1 or lacunary Wells Dawson increased stepwise from 0 to 10^{-5} M with increments of 10^{-6} M.

Luminescence spectroscopy

Time-resolved luminescence spectra were recorded on an Edinburgh Instruments FS920 spectrofluorimeter. Spectra were recorded with 10^{-4} M Eu-Wells Dawson POM concentration in an unbuffered solution with a pH varying from 6.95 to 7.37. The concentration of protein augmented stepwise from 0 to 10^{-4} M.
Steady state luminescence spectra were recorded on an Edinburgh Instruments FS900 steady state spectrofluorimeter. Spectra were recorded with 10^{-4} M Eu(III)-Wells-Dawson POM concentration in a 1 mM phosphate buffer of pH 7.4, monitoring the emission at 613 nm. The concentration of protein increased stepwise from 0 to 10^{-4} M.

Electrophoresis

Solutions containing 0.02 mM of protein were mixed with $K_{15}H[Zr(\alpha_2\text{-}P_2W_{17}O_{61})_2]\cdot 25H_2O$ in phosphate buffer (10.0 mM, pH 7.4). Samples were incubated at 60 °C and aliquots were taken at different time increments up to 7 days and analyzed with SDS-PAGE. SDS-PAGE gels were stained with silver staining and an image of each gel was taken with a GelDoc EZ Imager (Bio-Rad). Alternatively, proteins in SDS-PAGE gels were electroblotted to PVDF membrane, stained with coommasie brilliant blue and sequenced by capillary Edman degradation on a 491 Procise cLC protein sequencer (Applied Biosystems, Foster City, CA, USA).

Acknowledgements

K.S. thanks the FWO Flanders for the doctoral fellowship. V.G. acknowledges KU Leuven for the doctoral fellowship. G. A. thanks the FWO Flanders for the post-doctoral fellowship. G. B. acknowledges the FNRS (FRFC 2010 : 2.4592.10F) and the Van Buuren Foundation for the funding. P.P. and E.M. received financial support from the FWO Flanders and the Concerted Research Actions (GOA) of the KU Leuven. T.N.P.V. thanks KU Leuven (OT/13/060) and FWO Flanders for the financial support.

Keywords: polyoxometalate • hydrolysis • interaction • HSA • Zr(IV)

[1] A. Radzicka and R. Wolfenden, *Journal of the American Chemical Society* **1996**, *118*, 6105-6109.

[2] A. Fontana, P. P. de Laureto, B. Spolaore, E. Frare, P. Picotti and M. Zambonin, *Acta Biochimica Polonica* **2004**, *51*, 299-321.

[3] L. Zhu, R. Bakhtiar and N. M. Kostic, *Journal of Biological Inorganic Chemistry* **1998**, *3*, 383-391.

[4] A. Fontana, M. Zambonin, P. P. deLaureto, V. DeFilippis, A. Clementi and E. Scaramella, *Journal of Molecular Biology* **1997**, *266*, 223-230.

[5] K. B. Grant and M. Kassai, *Current Organic Chemistry* **2006**, *10*, 1035-1049.

[6] a) L. G. Zhu, L. Qin, T. N. Parac and N. M. Kostic, *Journal of the American Chemical Society* **1994**, *116*, 5218-5224; b) N. M. Milovic and N. M. Kostic, *Journal of the American Chemical Society* **2002**, *124*, 4759-4769.

[7] N. M. Milovic, L. M. Dutca and N. M. Kostic, *Chemistry-a European Journal* **2003**, *9*, 5097-5106.

[8] J. W. Jeon, S. J. Son, C. E. Yoo, I. S. Hong and J. Suh, *Bioorganic & Medicinal Chemistry* **2003**, *11*, 2901-2910.

[9] a) C. E. Yoo, P. S. Chae, J. E. Kim, E. J. Jeong and J. Suh, *Journal of the American Chemical Society* **2003**, *125*, 14580-14589; b) M. S. Kim and J. Suh, *Bulletin of the Korean Chemical Society* **2005**, *26*, 1911-1920.

[10] a) V. Goovaerts, K. Stroobants, G. Absillis and T. N. Parac-Vogt, *Physical Chemistry Chemical Physics* **2013**, *15*, 18378-18387; b) K. Stroobants, E. Moelants, H. G. T. Ly, P. Proost, K. Bartik and T. N. Parac-Vogt, *Chemistry-a European Journal* **2013**, *19*, 2848-2858.

[11] A. Proust, R. Thouvenot and P. Gouzerh, *Chemical Communications* **2008**, 1837-1852.

[12] J. T. Rhule, C. L. Hill and D. A. Judd, *Chemical Reviews* **1998**, *98*, 327-357.

[13] a) D. A. Judd, J. H. Nettles, N. Nevins, J. P. Snyder, D. C. Liotta, J. Tang, J. Ermolieff, R. F. Schinazi and C. L. Hill, *Journal of the American Chemical Society* **2001**, *123*, 886-897; b) K. Dan and T. Yamase, *Biomedicine & Pharmacotherapy* **2006**, *60*, 169-173.

[14] X. Wang, J. Liu, J. Li, Y. Yang, J. Liu, B. Li and M. T. Pope, *Journal of Inorganic Biochemistry* **2003**, *94*, 279-284.

[15] N. Fukuda, T. Yamase and Y. Tajima, *Biological & Pharmaceutical Bulletin* **1999**, *22*, 463-470.

[16] a) G. Zhang, B. Keita, C. T. Craescu, S. Miron, P. de Oliveira and L. Nadjo, *Journal of Physical Chemistry B* **2007**, *111*, 11253-11259; b) G. J. Zhang, B. Keita, J. C. Brochon, P. de Oliveira, L. Nadjo, C. T. Craescu and S. Miron, *Journal of Physical Chemistry B* **2007**, *111*, 1809-1814; c) G. J. Zhang, B. Keita, C. T. Craescu, S. Miron, P. de Oliveira and L. Nadjo, *Biomacromolecules* **2008**, *9*, 812-817; d) L. Zheng, Y. Ma, G. J. Zhang, J. N. Yao, B. S. Bassil, U. Kortz, B. Keita, P. de Oliveira, L. Nadjo, C. T. Craescu and S. Miron, *European Journal of Inorganic Chemistry* **2009**, 5189-5193; e) L. Zheng, Y. Ma, G. J. Zhang, J. N. Yao, B. Keita and L. Nadjo, *Physical Chemistry Chemical Physics* **2010**, *12*, 1299-1304; f) G. Hungerford, K. Suhling and M. Green, *Photochemical & Photobiological Sciences* **2008**, *7*, 734-737; g) G. Hungerford, F. Hussain, G. R. Patzke and M. Green, *Physical Chemistry Chemical Physics* **2010**, *12*, 7266-7275.

[17] P. H. Ho, E. Breynaert, C. E. A. Kirschhock and T. N. Parac-Vogt, *Dalton Transactions* **2011**, *40*, 295-300.

[18] a) N. Steens, A. M. Ramadan, G. Absillis and T. N. Parac-Vogt, *Dalton Transactions* **2010**, *39*, 585-592; b) E. Cartuyvels, G. Absillis and T. N. Parac-Vogt, *Chemical Communications* **2008**, 85-87; c) G. Absillis, E. Cartuyvels, R. Van Deun and T. N. Parac-Vogt, *Journal of the American Chemical Society* **2008**, *130*, 17400-17408; d) G. Absillis, R. Van Deun and T. N. Parac-Vogt, *Inorganic Chemistry* **2011**, *50*, 11552-11560.

[19] a) P. H. Ho, K. Stroobants and T. N. Parac-Vogt, *Inorganic Chemistry* **2011**, *50*, 12025-12033; b) P. H. Ho, T. Mihaylov, K. Pierloot and T. N. Parac-Vogt, *Inorganic Chemistry* **2012**, *51*, 8848-8859.

[20] K. Stroobants, P. H. Ho, E. Moelants, P. Proost and T. N. Parac-Vogt, *Journal of Inorganic Biochemistry* **2014,** DOI: 10.1016/j.jinorgbio.2014.03.006.

[21] G. Absillis and T. N. Parac-Vogt, *Inorganic Chemistry* **2012**, *51*, 9902-9910.

[22] C. Boglio, K. Micoine, P. Rémy, B. Hasenknopf, S. Thorimbert, E. Lacôte, M. Malacria, C. Afonso and J.-C. Tabet, *Chemistry – A European Journal* **2007**, *13*, 5426-5432.

[23] a) G. Al-Kadamany, S. S. Mal, B. Milev, B. G. Donoeva, R. I. Maksimovskaya, O. A. Kholdeeva and U. Kortz, *Chemistry-a European Journal* **2010**, *16*, 11797-11800; b) O. A. Kholdeeva, G. M. Maksimov, R. I. Maksimovskaya, M. P. Vanina, T. A. Trubitsina, D. Y. Naumov, B. A. Kolesov, N. S. Antonova, J. J. Carbo and J. M. Poblet, *Inorganic Chemistry* **2006**, *45*, 7224-7234.

[24] a) M. Carraro, N. Nsouli, H. Oelrich, A. Sartorel, A. Soraru, S. S. Mal, G. Scorrano, L. Walder, U. Kortz and M. Bonchio, *Chemistry-a European Journal* **2011**, *17*, 8371-8378; b) S. S. Mal, N. H. Nsouli, M. Carraro, A. Sartorel, G. Scorrano, H. Oelrich, L. Walder, M. Bonchio and U. Kortz, *Inorganic Chemistry* **2010**, *49*, 7-9.

[25] Y. Kikukawa, S. Yamaguchi, K. Tsuchida, Y. Nakagawa, K. Uehara, K. Yamaguchi and N. Mizuno, *Journal of the American Chemical Society* **2008**, *130*, 5472-5478.

[26] a) S. Vanhaecht, G. Absillis and T. N. Parac-Vogt, *Dalton Transactions* **2013**, *42*, 15437-15446; b) H. G. T. Ly, G. Absillis and T. N. Parac-Vogt, *Dalton Transactions* **2013**, *42*, 10929-10938; c) H. G. T. Ly, G. Absillis, S. R. Bajpe, J. A. Martens and T. N. Parac-Vogt, *European Journal of Inorganic Chemistry* **2013**, *2013*, 4601-4611.

[27] K. Stroobants, G. Absillis, E. Moelants, P. Proost and T. N. parac-Vogt, *Chemistry - A European Journal* **2013,** DOI: 10.1002/chem.201303622.

[28] a) M. N. Sokolov, N. V. Izarova, E. V. Peresypkina, D. A. Mainichev and V. P. Fedin, *Inorganica Chimica Acta* **2009**, *362*, 3756-3762; b) M. N. Sokolov, N. V. Izarova, E. V. Peresypkina, A. V. Virovets and V. P. Fedin, *Russian Chemical Bulletin* **2009**, *58*, 507-512; c) Y. Saku, Y. Sakai and K. Nomiya, *Inorganica Chimica Acta* **2010**, *363*, 967-974.

[29] a) C. Boglio, B. Hasenknopf, G. Lenoble, P. Remy, P. Gouzerh, S. Thorimbert, E. Lacote, M. Malacria and R. Thouvenot, *Chemistry-a European Journal* **2008**, *14*, 1532-1540; b) N. Dupre, P. Remy, K. Micoine, C. Boglio, S. Thorimbert, E. Lacote, B. Hasenknopf and M. Malacria, *Chemistry-a European Journal* **2010**, *16*, 7256-7264.

[30] G. Zhang, B. Keita, C. T. Craescu, S. Miron, P. de Oliveira and L. Nadjo, *Biomacromolecules* **2008**, *9*, 812-817.

[31] J. E. Ladbury and M. L. Doyle in *Biocalorimetry 2 Applications of calorimetry in the biological sciences*, *Vol.* John Wiley & Sons Ltd, Chichester, **2004**.

[32] Y. Moriyama, D. Ohta, K. Hachiya, Y. Mitsui and K. Takeda, *Journal of Protein Chemistry* **1996**, *15*, 265-272.

[33] a) G. Zhang, B. Keita, J.-C. Brochon, P. de Oliveira, L. Nadjo, C. T. Craescu and S. Miron, *Journal of Physical Chemistry B* **2007**, *111*, 1809-1814; b) L. Zheng, Y. Ma, G. Zhang, J. Yao, B. Keita and L. Nadjo, *Physical Chemistry Chemical Physics* **2010**, *12*, 1299-1304.

[34] C. Zhang, L. Bensaid, D. McGregor, X. Fang, R. C. Howell, B. Burton-Pye, Q. Luo, L. Todaro and L. C. Francesconi, *Journal of Cluster Science* **2006**, *17*, 389-425.

[35] R. M. Supkowski and W. D. Horrocks, *Inorganica Chimica Acta* **2002**, *340*, 44-48.

[36] C. A. Kodaira, H. F. Brito, O. L. Malta and O. A. Serra, *Journal of Luminescence* **2003**, *101*, 11-21.

[37] a) S. Lis and S. But, *Journal of Alloys and Compounds* **2000**, *300*, 370-376; b) S. Lis and S. But, *Rare Earths '98* **1999**, *315-3*, 431-438.

[38] M. Yashiro, Y. Kawakami, J. I. Taya, S. Arai and Y. Fujii, *Chemical Communications* **2009**, 1544-1546.

[39] V. Rajendiran, M. Palaniandavar, P. Swaminathan and L. Uma, *Inorganic Chemistry* **2007**, *46*, 10446-10448.

[40] S. Sugio, A. Kashima, S. Mochizuki, M. Noda and K. Kobayashi, *Protein Engineering* **1999**, *12*, 439-446.

[41] M. Dockal, D. C. Carter and F. Ruker, *Journal of Biological Chemistry* **1999**, *274*, 29303-29310.

[42] A. P. Ginsberg, *Inorganic Synthesis*, **1990**.

[43] C. N. Kato, A. Shinohara, K. Hayashi and K. Nomiya, *Inorganic Chemistry* **2006**, *45*, 8108-8119.

Received: ((will be filled in by the editorial staff))
Revised: ((will be filled in by the editorial staff))
Published online: ((will be filled in by the editorial staff))

DOI: 10.1002/chem.201xxxxxx

ChemPubSoc Europe

DOI: 10.1002/chem.201xxxxxx

CHEMISTRY
A European Journal
Full Paper

Entry for the Table of Contents

FULL PAPER

A multi-technique approach has been applied to identify the thermodynamic and kinetic parameters related to the regioselective hydrolysis of HSA promoted by the Wells-Dawson polyoxometalate (POM) $K_{15}H[Zr(\alpha_2\text{-}P_2W_{17}O_{61})_2]$. All interaction studies are in accordance with combined POM dominated binding and interactions governed by metal anchoring. A detailed kinetic study has evidenced that the regioselectivity of $K_{15}H[Zr(\alpha_2\text{-}P_2W_{17}O_{61})_2]$ is fixed even at high POM concentrations and upon prolonged reaction times.

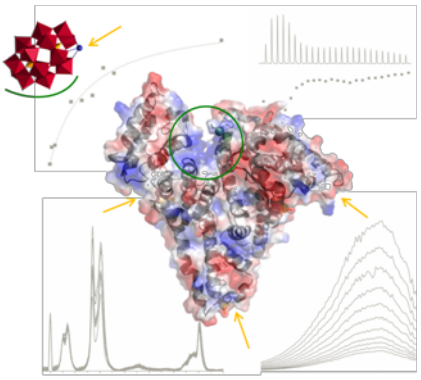

Polyoxometalate reactivity

*Karen Stroobants, Vincent Goovaerts, Gregory Absillis, Gilles Bruylants, Eva Moelants, Paul Proost and Tatjana N. Parac-Vogt**

■■ – ■■

Molecular origin of the hydrolytic activity and fixed regioselectivity of a Zr(IV)-substituted polyoxotungstate as artificial protease

[1] A. Radzicka and R. Wolfenden, *Journal of the American Chemical Society* **1996**, *118*, 6105-6109.
[2] A. Fontana, P. P. de Laureto, B. Spolaore, E. Frare, P. Picotti and M. Zambonin, *Acta Biochimica Polonica* **2004**, *51*, 299-321.
[3] L. Zhu, R. Bakhtiar and N. M. Kostic, *Journal of Biological Inorganic Chemistry* **1998**, *3*, 383-391.
[4] A. Fontana, M. Zambonin, P. P. deLaureto, V. DeFilippis, A. Clementi and E. Scaramella, *Journal of Molecular Biology* **1997**, *266*, 223-230.
[5] K. B. Grant and M. Kassai, *Current Organic Chemistry* **2006**, *10*, 1035-1049.
[6] a) L. G. Zhu, L. Qin, T. N. Parac and N. M. Kostic, *Journal of the American Chemical Society* **1994**, *116*, 5218-5224; b) N. M. Milovic and N. M. Kostic, *Journal of the American Chemical Society* **2002**, *124*, 4759-4769.
[7] N. M. Milovic, L. M. Dutca and N. M. Kostic, *Chemistry-a European Journal* **2003**, *9*, 5097-5106.
[8] J. W. Jeon, S. J. Son, C. E. Yoo, I. S. Hong and J. Suh, *Bioorganic & Medicinal Chemistry* **2003**, *11*, 2901-2910.
[9] a) C. E. Yoo, P. S. Chae, J. E. Kim, E. J. Jeong and J. Suh, *Journal of the American Chemical Society* **2003**, *125*, 14580-14589; b) M. S. Kim and J. Suh, *Bulletin of the Korean Chemical Society* **2005**, *26*, 1911-1920.
[10] a) V. Goovaerts, K. Stroobants, G. Absillis and T. N. Parac-Vogt, *Physical Chemistry Chemical Physics* **2013**, *15*, 18378-18387; b) K. Stroobants, E. Moelants, H. G. T. Ly, P. Proost, K. Bartik and T. N. Parac-Vogt, *Chemistry-a European Journal* **2013**, *19*, 2848-2858.
[11] A. Proust, R. Thouvenot and P. Gouzerh, *Chemical Communications* **2008**, 1837-1852.
[12] J. T. Rhule, C. L. Hill and D. A. Judd, *Chemical Reviews* **1998**, *98*, 327-357.
[13] a) D. A. Judd, J. H. Nettles, N. Nevins, J. P. Snyder, D. C. Liotta, J. Tang, J. Ermolieff, R. F. Schinazi and C. L. Hill, *Journal of the American Chemical Society* **2001**, *123*, 886-897; b) K. Dan and T. Yamase, *Biomedicine & Pharmacotherapy* **2006**, *60*, 169-173.
[14] X. Wang, J. Liu, J. Li, Y. Yang, J. Liu, B. Li and M. T. Pope, *Journal of Inorganic Biochemistry* **2003**, *94*, 279-284.
[15] N. Fukuda, T. Yamase and Y. Tajima, *Biological & Pharmaceutical Bulletin* **1999**, *22*, 463-470.
[16] a) G. Zhang, B. Keita, C. T. Craescu, S. Miron, P. de Oliveira and L. Nadjo, *Journal of Physical Chemistry B* **2007**, *111*, 11253-11259; b) G. J. Zhang, B. Keita, J. C. Brochon, P. de Oliveira, L. Nadjo, C. T. Craescu and S. Miron, *Journal of Physical Chemistry B* **2007**, *111*, 1809-1814; c) G. J. Zhang, B. Keita, C. T. Craescu, S. Miron, P. de Oliveira and L. Nadjo, *Biomacromolecules* **2008**, *9*, 812-817; d) L. Zheng, Y. Ma, G. J. Zhang, J. N. Yao, B. S. Bassil, U. Kortz, B. Keita, P. de Oliveira, L. Nadjo, C. T. Craescu and S. Miron, *European Journal of Inorganic Chemistry* **2009**, 5189-5193; e) L. Zheng, Y. Ma, G. J. Zhang, J. N. Yao, B. Keita and L. Nadjo, *Physical Chemistry Chemical Physics* **2010**, *12*, 1299-1304; f) G. Hungerford, K. Suhling and M. Green, *Photochemical & Photobiological Sciences* **2008**, *7*, 734-737; g) G. Hungerford, F. Hussain, G. R. Patzke and M. Green, *Physical Chemistry Chemical Physics* **2010**, *12*, 7266-7275.
[17] P. H. Ho, E. Breynaert, C. E. A. Kirschhock and T. N. Parac-Vogt, *Dalton Transactions* **2011**, *40*, 295-300.
[18] a) N. Steens, A. M. Ramadan, G. Absillis and T. N. Parac-Vogt, *Dalton Transactions* **2010**, *39*, 585-592; b) E. Cartuyvels, G. Absillis and T. N. Parac-Vogt, *Chemical Communications* **2008**, 85-87; c) G. Absillis, E. Cartuyvels, R. Van Deun and T. N. Parac-Vogt, *Journal of the American Chemical Society* **2008**, *130*, 17400-17408; d) G. Absillis, R. Van Deun and T. N. Parac-Vogt, *Inorganic Chemistry* **2011**, *50*, 11552-11560.
[19] a) P. H. Ho, K. Stroobants and T. N. Parac-Vogt, *Inorganic Chemistry* **2011**, *50*, 12025-12033; b) P. H. Ho, T. Mihaylov, K. Pierloot and T. N. Parac-Vogt, *Inorganic Chemistry* **2012**, *51*, 8848-8859.
[20] K. Stroobants, P. H. Ho, E. Moelants, P. Proost and T. N. Parac-Vogt, *Journal of Inorganic Biochemistry* **2014,** DOI: 10.1016/j.jinorgbio.2014.03.006.
[21] G. Absillis and T. N. Parac-Vogt, *Inorganic Chemistry* **2012**, *51*, 9902-9910.
[22] C. Boglio, K. Micoine, P. Rémy, B. Hasenknopf, S. Thorimbert, E. Lacôte, M. Malacria, C. Afonso and J.-C. Tabet, *Chemistry – A European Journal* **2007**, *13*, 5426-5432.
[23] a) G. Al-Kadamany, S. S. Mal, B. Milev, B. G. Donoeva, R. I. Maksimovskaya, O. A. Kholdeeva and U. Kortz, *Chemistry-a European Journal* **2010**, *16*, 11797-11800; b) O. A. Kholdeeva, G. M. Maksimov, R. I. Maksimovskaya, M. P. Vanina, T. A. Trubitsina, D. Y. Naumov, B. A. Kolesov, N. S. Antonova, J. J. Carbo and J. M. Poblet, *Inorganic Chemistry* **2006**, *45*, 7224-7234.
[24] a) M. Carraro, N. Nsouli, H. Oelrich, A. Sartorel, A. Soraru, S. S. Mal, G. Scorrano, L. Walder, U. Kortz and M. Bonchio, *Chemistry-a European Journal* **2011**, *17*, 8371-8378; b) S. S. Mal, N. H. Nsouli, M. Carraro, A. Sartorel, G. Scorrano, H. Oelrich, L. Walder, M. Bonchio and U. Kortz, *Inorganic Chemistry* **2010**, *49*, 7-9.
[25] Y. Kikukawa, S. Yamaguchi, K. Tsuchida, Y. Nakagawa, K. Uehara, K. Yamaguchi and N. Mizuno, *Journal of the American Chemical Society* **2008**, *130*, 5472-5478.
[26] a) S. Vanhaecht, G. Absillis and T. N. Parac-Vogt, *Dalton Transactions* **2013**, *42*, 15437-15446; b) H. G. T. Ly, G. Absillis and T. N. Parac-Vogt, *Dalton Transactions* **2013**, *42*, 10929-10938; c) H. G. T. Ly, G. Absillis, S. R. Bajpe, J. A. Martens and T. N. Parac-Vogt, *European Journal of Inorganic Chemistry* **2013**, *2013*, 4601-4611.
[27] K. Stroobants, G. Absillis, E. Moelants, P. Proost and T. N. parac-Vogt, *Chemistry - A European Journal* **2013,** DOI: 10.1002/chem.201303622.
[28] a) M. N. Sokolov, N. V. Izarova, E. V. Peresypkina, D. A. Mainichev and V. P. Fedin, *Inorganica Chimica Acta* **2009**, *362*, 3756-3762; b) M. N. Sokolov, N. V. Izarova, E. V. Peresypkina, A. V. Virovets and V. P. Fedin, *Russian Chemical Bulletin* **2009**, *58*, 507-512; c) Y. Saku, Y. Sakai and K. Nomiya, *Inorganica Chimica Acta* **2010**, *363*, 967-974.
[29] a) C. Boglio, B. Hasenknopf, G. Lenoble, P. Remy, P. Gouzerh, S. Thorimbert, E. Lacote, M. Malacria and R. Thouvenot, *Chemistry-a European Journal* **2008**, *14*, 1532-1540; b) N. Dupre, P. Remy, K. Micoine, C. Boglio, S. Thorimbert, E. Lacote, B. Hasenknopf and M. Malacria, *Chemistry-a European Journal* **2010**, *16*, 7256-7264.
[30] G. Zhang, B. Keita, C. T. Craescu, S. Miron, P. de Oliveira and L. Nadjo, *Biomacromolecules* **2008**, *9*, 812-817.
[31] J. E. Ladbury and M. L. Doyle in *Biocalorimetry 2 Applications of calorimetry in the biological sciences*, *Vol.* John Wiley & Sons Ltd, Chichester, **2004**.
[32] Y. Moriyama, D. Ohta, K. Hachiya, Y. Mitsui and K. Takeda, *Journal of Protein Chemistry* **1996**, *15*, 265-272.
[33] a) G. Zhang, B. Keita, J.-C. Brochon, P. de Oliveira, L. Nadjo, C. T. Craescu and S. Miron, *Journal of Physical Chemistry B* **2007**, *111*, 1809-1814; b) L. Zheng, Y. Ma, G. Zhang, J. Yao, B. Keita and L. Nadjo, *Physical Chemistry Chemical Physics* **2010**, *12*, 1299-1304.
[34] C. Zhang, L. Bensaid, D. McGregor, X. Fang, R. C. Howell, B. Burton-Pye, Q. Luo, L. Todaro and L. C. Francesconi, *Journal of Cluster Science* **2006**, *17*, 389-425.
[35] R. M. Supkowski and W. D. Horrocks, *Inorganica Chimica Acta* **2002**, *340*, 44-48.
[36] C. A. Kodaira, H. F. Brito, O. L. Malta and O. A. Serra, *Journal of Luminescence* **2003**, *101*, 11-21.
[37] a) S. Lis and S. But, *Journal of Alloys and Compounds* **2000**, *300*, 370-376; b) S. Lis and S. But, *Rare Earths '98* **1999**, *315-3*, 431-438.
[38] M. Yashiro, Y. Kawakami, J. I. Taya, S. Arai and Y. Fujii, *Chemical Communications* **2009**, 1544-1546.
[39] V. Rajendiran, M. Palaniandavar, P. Swaminathan and L. Uma, *Inorganic Chemistry* **2007**, *46*, 10446-10448.
[40] S. Sugio, A. Kashima, S. Mochizuki, M. Noda and K. Kobayashi, *Protein Engineering* **1999**, *12*, 439-446.
[41] M. Dockal, D. C. Carter and F. Ruker, *Journal of Biological Chemistry* **1999**, *274*, 29303-29310.
[42] A. P. Ginsberg, *Inorganic Synthesis*, **1990**, p.
[43] C. N. Kato, A. Shinohara, K. Hayashi and K. Nomiya, *Inorganic Chemistry* **2006**, *45*, 8108-8119.